Pergamon

Geothermics Vol. 27, No. 4, pp. 445–467, 1998
© 1998 CNR
Elsevier Science Ltd
Printed in Great Britain. All rights reserved
0375–6505/98 $19.00+0.00

PII: S0375-6505(98)00022-4

THE THERMAL SPRINGS OF BOCKFJORD, SVALBARD: OCCURRENCE AND MAJOR ION HYDROCHEMISTRY

DAVID BANKS,*¶ RONALD S. SLETTEN,† SYLVI HALDORSEN,‡
BARRIE DALE,§ MICHAEL HEIM‡ and BERIT SWENSEN‡

**Norges Geologiske Undersøkelse* (*Geological Survey of Norway*), *Postboks* 3006 *Lade*,
*N*7002 *Trondheim*, *Norway*.
†*Quaternary Research Center*, *Box* 351360, *University of Washington*, *Seattle*,
Washington 98195-1360, *U.S.A.*
‡*Department of Soil and Water Sciences*, *Norges Landbrukshøyskole*
(*Agricultural University of Norway*), *Postboks* 5028, *N*1432, *Ås*, *Norway*.
§*Department of Geology*, *University of Oslo*, *Postboks* 1047 *Blindern*, *N*0316 *Oslo*, *Norway*.

(*Received May* 1997; *accepted March* 1998)

Abstract—The Troll and Jotun thermal springs of northern Svalbard, with temperatures of up to 25.6°C, are derived from a major fault forming the junction between Devonian sandstones and Proterozoic marbles, mica schists and gneisses. The Troll waters are dominated by Na–HCO_3 compositions and the Jotun waters by Na–Cl compositions. The 'pristine' thermal water source has a sub-neutral pH and is highly reducing. Taken at face value, common geothermometers suggest temperatures at depth of 130–180°C for the Troll springs (corresponding to a depth of 1.6–2.3 km), with 10–30% thermal water diluted by 70–90% cold water. Such geothermometers may, however, be inappropriate to the cool, high CO_2 waters of Bockfjord, and real temperatures at depth and dilution factors are probably considerably lower. The salinity of the thermal water appears to be only partially derived from water–rock interaction; Br/Cl ratios suggest that seawater or possibly evaporites may be a source of chloride salinity. © 1998 *CNR. Published by Elsevier Science Ltd. All rights reserved*

Key words: thermal waters, geochemistry, Svalbard, Spitsbergen.

INTRODUCTION

The two groups of thermal springs at Bockfjord, the Troll springs and the Jotun springs (Fig. 1), at almost 80°N latitude on Svalbard, probably represent the northernmost documented subaerial thermal springs in the world. In July 1996 a multidisciplinary team of scientists visited the spring sites to examine the hydrochemistry, flow regime, isotopic composition, geological situation and microbiology of the springs with the following objectives:

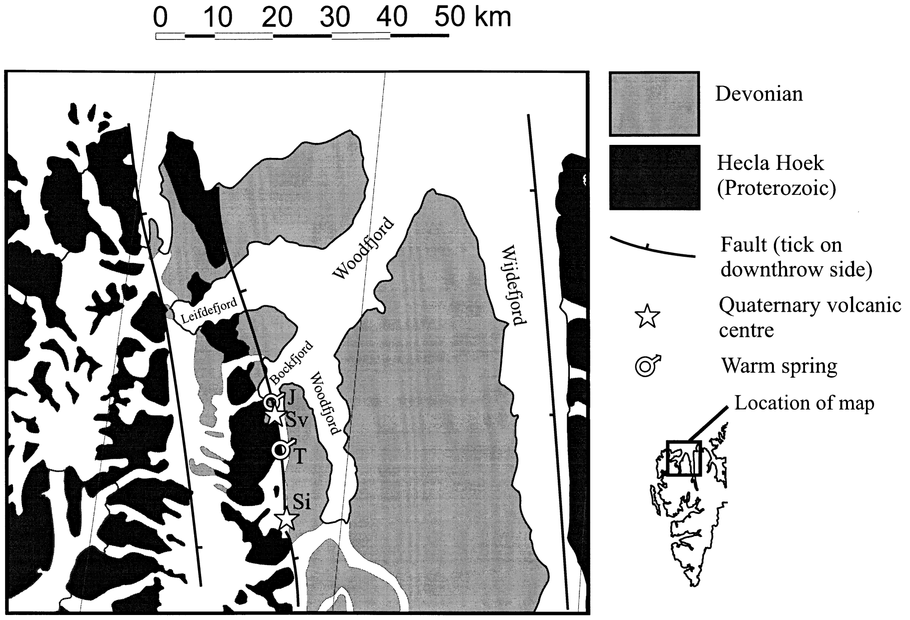

Fig. 1. Sketch map of the Woodfjord area of northern Svalbard. J = Jotun springs, Sv = Sverrefjellet, T = Troll springs, Si = Sigurdfjellet. White areas represent glaciated terrain or terrain covered by Quaternary (moraine/sandur) deposits. Inset shows map of Spitsbergen with location of main map.

1. To document and understand a unique natural phenomenon which, although currently in a near-pristine state, is likely to become increasingly visited by tourists and scientists in the near future.
2. To increase our understanding of groundwater recharge and discharge processes in deeply permafrosted terrains (see e.g. Lauritzen, 1991; Haldorsen and Lauritzen, 1993).
3. To explore novel ways of obtaining information on past climatic variations on Svalbard from the isotopic signature preserved in the springs' travertine deposits.

This paper seeks to document and interpret the hydrochemistry of major and selected minor elements in the spring waters. Future papers will address the trace element and isotope chemistry of the waters, host rocks and travertine deposits, and the interpretation of the hydrogeological regime.

THE THERMAL SPRINGS OF SVALBARD

In a permafrost terrain, where the annual average surface temperature is <0°C, any persistent groundwater spring may be regarded as thermal according to strict definitions. There are typically three types of springs on Svalbard:

Type 1: during summer, melting of permafrost in the active layer leads to the creation of very shallow groundwater systems and springs, discharging at temperatures of near 0°C.

Type 2: springs derived from systems of sub-permafrost groundwater. Under much of Svalbard, permafrost may exceed 300 m thickness (Orvin, 1944). Groundwater recharge is believed to take place below warm-based parts of glaciers, where permafrost is absent (Liestøl, 1976; Lauritzen, 1991; Haldorsen and Lauritzen, 1993; Lauritzen and Bottrell, 1994). Groundwater flows beneath the thick permafrost layer to discharge at springs, which may be high-discharge karstic springs or low-discharge springs that may form pingos (frost mounds), where there are open taliks in the permafrost. The location of the base of the permafrost and the temperature of the groundwater depend on a complex interplay of several factors such as surface climate and topography, geothermal heat flow, groundwater flow and frictional heat generated by groundwater flow. Lauritzen (1991) and Haldorsen and Lauritzen (1993) note that much sub-permafrost groundwater discharges at temperatures of around 1–4°C.

Type 3: Svalbard boasts a number of springs that are more impressively thermal, often with significant discharges (Orvin, 1944). Examples of H_2S-rich, saline springs with temperatures of up to 15°C were described at Fisneset ('Fart Point') by Lauritzen and Bottrell (1994). These lie on the Hornsund fault zone of Southern Svalbard and the salinity appears to be derived from a deep thermal brine rather than modern sea water. The Troll and Jotun springs bear many similarities to the Fisneset springs but lie much further north and are considerably hotter.

THE BOCKFJORD SPRINGS

History

The springs are believed to have been documented first in the late 19th century, and they are described in some detail by Hoel and Holtedahl (1911, 1913) and Hoel (1914). These authors measured water temperatures of 24.5°C at the Jotun springs and up to 28.3°C at the Troll springs. They also provide details of some chemical analyses performed at that time (Table 1), which are of interest in comparison with the current analytical suite. Hoel and Holtedahl (1911) also observe that the waters are of dominantly sodium bicarbonate character.

Geological setting

The springs occur almost on the line of a major fault that appears to follow the western shore of Bockfjord. The fault has a large downthrow on the eastern side and forms the

Table 1. Composition of Troll and Jotun springs, Bockfjord, according to Hoel and Holtedahl (1911)

	Troll Springs No. 3	Jotun Spring No. 1	Jotun Spring No. 2
Total mineral content (mg/L)	988	2410	1456
Non-volatile mineral content (mg/L)	780	2178	1256
SO_4 (mg/L)	36	104	61
Cl (mg/L)	122	779	419
Ca (mg/L)	109	114	100
Mg (mg/L)	41	34	28

western boundary of a major graben structure, bringing the Devonian 'Old Red' sandstones and siltstones of the Wood Bay formation into contact with the Precambrian Hecla Hoek complex (Gjelsvik, 1979; Hjelle, 1993). The Hecla Hoek consists of a ca. 2 km wide outcrop of limestone and dolomite marbles in the east (adjacent to the fault), overlying a thick sequence of gneisses and migmatites that outcrop further west. The complex also includes phyllites, mica schists and metadolerites and is believed to be of mid–late Proterozoic age.

The Troll springs appear to emerge from brecciated fine-grained marbles of the Hecla Hoek complex, although an apparent outcrop of greenish basal Devonian sandstones can be observed in the shoreline several tens of metres east of Troll Spring Area 1. The geology of the Jotun Spring area is more difficult to interpret. Outcrops of Hecla Hoek marble are found a short distance below the springs although much of the frost-shattered material immediately around the springs is mica schist, also from the Hecla Hoek. Gee and Moody-Stuart (1966) describe the occurrence of Devonian sandstones on the coast north of Sverrefjell.

The Bockfjord area exhibits significant evidence of geologically recent crustal uplift, mantle lithosphere thinning and volcanism (Vågnes and Amundsen, 1993). The main phase of uplift and volcanism was in the Neogene, resulting in tholeiitic basalt caps to several of the mountains around Bockfjord. A later phase of alkaline olivine basalt and breccia eruption occurred near Bockfjord in the Quaternary, most notably from the volcanic centre of Sverrefjell, between the Troll and Jotun springs (Fig. 1). The volcanic centres of Sverrefjell and Sigurdfjell also lie on the same graben boundary fault as the springs. These volcanoes may have been active as recently as the last interstadial (Skjelkvåle *et al.*, 1989).

Vågnes and Amundsen (1993) suggest a geothermal heat-flow anomaly extending south from Yermak to Bockfjord, with a heat flow at Bockfjord of some 130 mW/m^2. Xenolithic evidence from Quaternary volcanism at Bockfjord suggests temperatures of 550°C at 7 km depth (Amundsen *et al.*, 1988), corresponding to a temperature gradient of some 0.079°C/m.

The age of the springs themselves is unknown. W.B. Harland and M.J. Hambrey are recorded by Langangen (1979) as opining that the springs are unlikely to be older than 4–6500 years. However, if Liestøl (1976) is correct in his theory that many springs and pingos on Svalbard first formed below sea-level, the springs might be older. They might even be as old as the volcanoes and may have formed subglacial spring outlets during the maximum of the last glaciation, as well as submarine spring outlets during the periods of high sea-level.

The Troll springs can be seen to occur below a fossil shore line, and at the same topographic level as apparently marine clays. One should not, however, conclude that the springs only became 'activated' on their post-glacial emergence from the sea. It is also possible that the springs may have survived marine inundation at times of higher sea-level. Submarine thermal springs are known today from the Tempelfjord area of Svalbard (Hoel and Holtedahl, 1911, 1913).

Spring morphology

The mountains to the south and west of Bockfjord are heavily glaciated. Lobes of glacier extend down almost to sea-level at the southern ends of Bockfjord and Woodfjord, with associated terminal moraine complexes and sandurs (outwash plains) with braided river systems. Smaller glacial lobes also extend almost to sea-level from side valleys along the western side of Bockfjord.

There are six discrete areas of travertine deposition associated with groups of active thermal springs at the Troll springs area. The spring areas are numbered 1 to 6 from the south. The springs typically deposit wide, shallowly concave, basin complexes of travertine, each basin with a low wall. The hottest waters emerge at the top of the basin complex (the so called A position, Fig. 2) and cascade down through the basin complex, often seeping into the travertine near the base of the complex. Below the basin complex, sheets of massive travertine breccia tend to occur. This presumably represents frost-shattered material cemented by the carbonate-saturated thermal groundwaters seeping through it. The thermal waters may re-emerge on their way down to the fjord at B and C positions or they may not re-emerge until the level of the sandur at the southern end of the fjord (D position). The spring nomenclature is such that 3A2 means 'the second spring of the third spring area from the south, A position spring'.

The top of the travertine deposits of Spring Area 6 is topographically higher than areas 1–5, but no active spring emerges from A position. Two thermal springs emerge lower down the travertine deposits in what is strictly a B position. As these are highest level waters of spring area 6, they are, for the purposes of this paper, designated 6A1 and 6A2.

A seventh fossil (inactive) spring area is observed between areas 5 and 6 at a considerably higher topographic level. It is argued that the two northern Spring Areas (6 and 7) were once active at times of greater groundwater head in the thermal system, enabling travertine systems to develop at a higher topographic level than today. It is of course possible that the effect is due to post-glacial emergence of the Svalbard coast and the actual head relative to sea-level has not changed. Nevertheless, in several spring areas, the size of the travertine basin complexes often appears disproportionately large relative to the flow of the current springs. This would indicate that groundwater heads and flow have genuinely been larger in the past, a conclusion supported by Hoel and Holtedahl (1911, 1913).

The Jotun springs have not developed any terraced travertine basins. They have rather developed huge convex mounds of travertine. At Spring Area 1 (east), three small springs (1JA1-3) emerge from the flattened top surface of the mound. At Spring Area 2 (west), no springs emerge from the top although one emerges from the flanks of the mound (designated 2JB). The remains of a third travertine area can be found at a higher level between Jotun Spring Areas 1 and 2.

Several springs appear to evolve gas bubbles (probably CO_2) regularly. The composition of the gas has not been determined, although at 3A1 the smell of H_2S can clearly be distinguished.

The flow from the springs is impossible to assess as much of the run-off from the A-

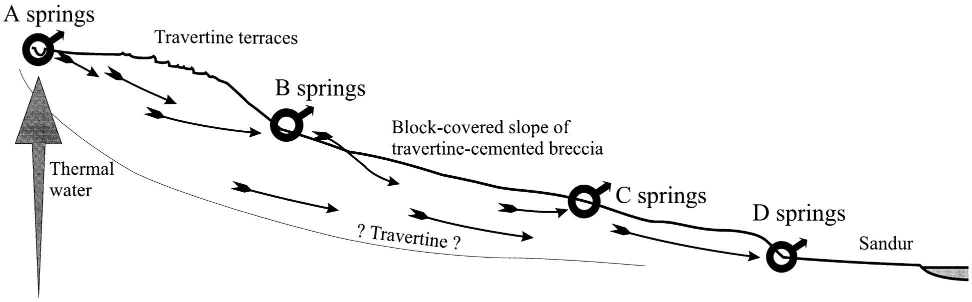

Fig. 2. Schematic cross-section of the structure and probable groundwater flow at the Troll springs site, Svalbard.

springs infiltrates directly into the permeable travertine as groundwater. It may be that only a minor proportion of the total spring flow is observed as surficial overflow from the springs.

Another thermal spring area has been reported by Otto Salvigsen, in a position between the Troll and Jotun springs, on the west of Bockfjord. Hitherto, it has not been documented in any detail.

SAMPLING PROGRAM

At almost all A-springs and a number of B-, C- and D-springs, pH, temperature and Eh were measured in the field. At selected springs (seven A-springs at Troll, two D-springs at Troll, and Jotun springs 1JA3 and 2JB), field analyses of alkalinity were carried out and samples were collected for laboratory analysis. The selected A springs include the hottest springs of each spring area (except area 4). Additionally, a cold spring between Spring Areas 3 and 4 at Troll was sampled (Sample K1). This is believed to be a permanent spring, as indicated by a verdant growth of spring moss, and is also believed to represent a discharge of non-thermal sub-permafrost groundwater (Type 2, see above), an interpretation confirmed by the rather mature hydrochemistry of the water. A sample was also taken from a thaw seepage from the active layer between Spring Areas 4 and 5 (Type 1, sample K2).

Field measurements of pH, temperature and Eh were made using a Yellow Springs YSI 3500 portable meter, calibrated regularly against buffer solutions of pH 4, 7 and 10. Alkalinity titrations were performed in the field using an Aquamerck kit with a pH = 4.3 mixed indicator. An average of three separate titrations was taken.

On the first day, 10 ml water samples for radon analysis were taken by injection into pre-filled vials containing a scintillation liquid (for method see Reimann *et al.*, 1996). These were returned by helicopter to be analysed at the National Radiation Protection Authority within three days, using scintillation counting. Duplicate samples were taken, whose analysis indicated the very good reproducibility of the technique, even at low radon concentrations.

For each sampled spring 2×100 mL samples of filtered water were taken in 100 mL polythene bottles. These were rinsed thrice with spring water prior to sampling and twice with filtered spring water. Samples were filtered with 0.45 μm Millipore filters. On arrival at the Geological Survey of Norway (NGU) laboratory, one flask of each sample was acidified with 0.5 mL/100 mL concentrated Suprapure (Merck) HNO_3 to remobilize and preserve any precipitated or adsorbed metals. This sample was then analysed for 32 parameters at NGU by Inductively Coupled Plasma spectroscopy [ICP–AES (Ødegård and Andreassen, 1987)]. The second flask of each sample was sent to the Norwegian Agricultural University (NLH) for anion analysis by Ion Chromatography (IC). The flask was then returned to NGU for confirmatory IC analysis.

RESULTS

XRD analysis of travertine material from three spring areas (Troll springs, areas 1, 3 and 5) confirmed it to be composed of almost pure calcite (Banks *et al.*, 1997b). No significant trace of either dolomite, aragonite or other major minerals was detected. The possible presence of minor amounts of monohydrocalcite, quartz and mica was indicated; the latter two could be detrital minerals.

The results of the water analyses are largely presented graphically in Figs 3–9 and in Tables 1 and 2. Ionic balances were found to be very good, all within 5%. At the Jotun springs, alkalinity could not be determined in the field for logistical reasons. In the diagrams and calculations, alkalinity for these has been estimated from the ion balance.

Three groups of thermal waters can be distinguished purely on the basis of Na, Ca, Mg, Cl, SO_4 and HCO_3: (i) the southern Troll Spring Areas 1, 2 and 3 with Na–(Ca)–HCO_3 composition, (ii) the northern Troll Spring Areas 5 and 6 with Na–HCO_3 waters, and (iii) the Jotun springs with Na–Cl waters. The waters within each group all have similar ionic composition in terms of proportions of major ions. Figure 3 shows pie diagrams of representatives of each water type, while Fig. 4 plots the waters on a Durov diagram. The northern Troll springs are more similar to the southern Troll springs than the Jotun springs. It is also noteworthy that the sub-permafrost non-thermal spring K1 displays a Ca–(Na)–HCO_3 composition that bears some resemblance to the southern Troll thermal waters. The thaw water K2 has a Ca–HCO_3 composition reflecting the dominant lithology in the active layer — shattered marble fragments.

Figures 5–9 and Table 2 show the relationship between various parameters and temperature and will not be commented in detail, although the reader's attention is drawn to the following observations:

1. pH and Eh tend to decrease with increasing temperature.
2. B, C and D springs generally exhibit lower temperatures and higher Eh values than A springs. Plots of Na vs. Cl (and also Mg and Sr vs. Cl, not shown) indicate a limited degree of proportionate dilution from warmer (A) to colder (D) springs (Fig. 8). A plot of Ca vs. Cl indicates, however, that calcium is being disproportionately attenuated (presumably due to calcite precipitation) to a much greater degree than chloride from the A to D springs.
3. Alkalinities of all the thermal Troll springs are high (around 13 meq/L). The calculated alkalinities of the Jotun springs are somewhat lower, around 7–10 meq/L.
4. The Na, K, SO_4 and Si concentrations all show extremely good correlations with each other, and to a lesser extent with Cl. Concentrations of these parameters in all the Troll springs are similar, independent of temperature, although elevated relative to K1 and K2. 2JB contains higher concentrations of these parameters, 1JA3 the highest of all.
5. The Na/Cl ratio in K2 is similar to that in sea-water (i.e. marine salts in precipitation). The other springs, including K1, exhibit significant non-marine excesses of Na.
6. Ca and, to a lesser extent Mg, show a better positive correlation with temperature than the parameters named in (4). Ca, Sr, Mg and alkalinity do not exhibit a particularly good covariation with the group of parameters Na, K and Si.
7. Br/Cl mass ratios for the thermal waters range from 0.0018 in 1JA3 to 0.0029 in 2A4i. In sea-water, the ratio varies from 0.00325 to 0.0043 (Horne, 1969; Michard *et al.*, 1996), with a typical value of 0.00347 being used by Edmunds (1996).
8. Significantly elevated levels of Fe and Mn occur in the hotter A springs (this may be related to low Eh).
9. Rn levels are replicable and are significantly lower in the thermal springs than in K1.
10. All thermal waters exhibit reasonably consistent but elevated Na/Si (ca. 10) and Mg/Ca (ca. 0.3) ratios compared with K1 and K2 (Fig. 9). The same applies to Sr/Ca (ca. 0.011) and Na/Ca (ca. 3) mass ratios (Table 2).
11. The thermal springs exhibit three groups of Na/K mass ratio (Fig. 9); the Jotun springs

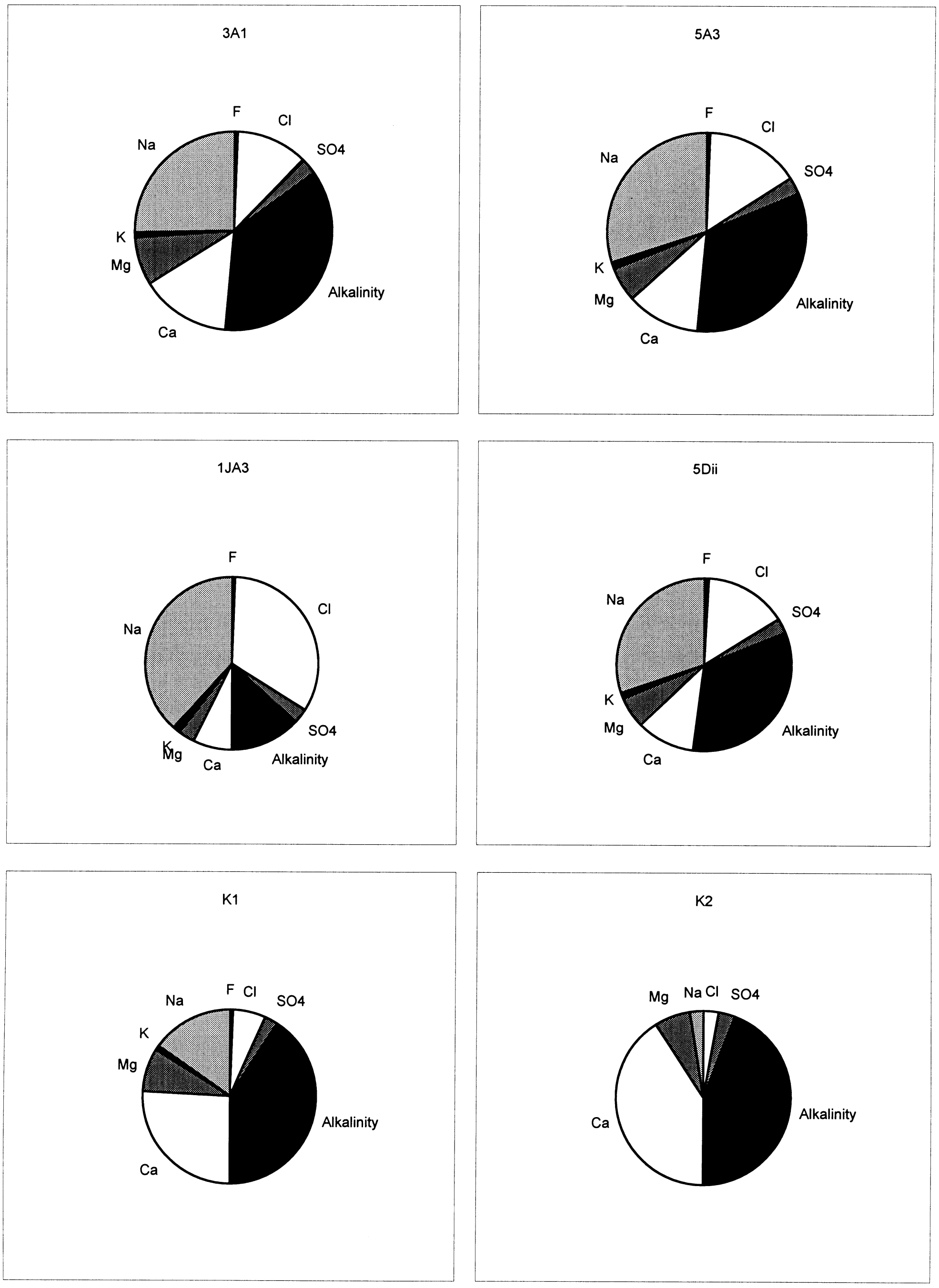

Fig. 3. Pie diagrams showing major ion composition of groundwaters from springs 3A1, 5A3, 1JA3, 5Dii, K1 and K2, Svalbard.

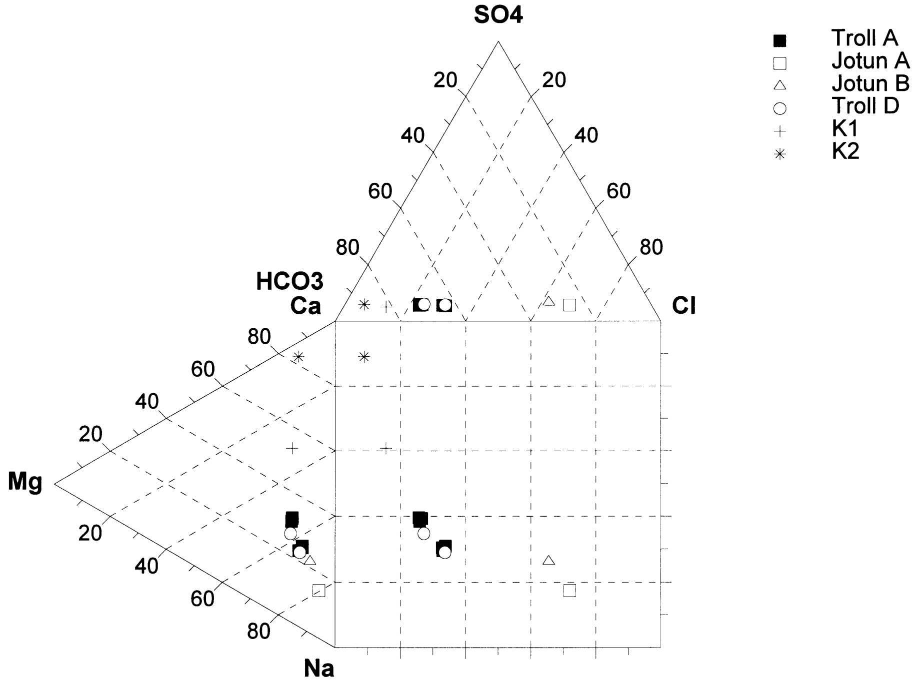

Fig. 4. Durov diagram showing the major-ion composition of groundwaters from the Troll and Jotun spring areas, Svalbard.

at around 13.5 to 15.5, the southern Troll springs between 16 and 16.5 and the northern Troll springs at around 17.5. This grouping suggests that Na/K ratios may be an interesting tool in the context of geothermometry.

INTERPRETATION

The thermal waters share some of the features exhibited by K1. This may imply either that some of the processes seen in the thermal waters can be explained by normal hydrochemical evolution occurring in the sub-permafrost zone, or that K1 includes a component of thermal water.

Observation (1) above suggests that 3A1 is the most ‘original’ of the Troll springs: it is the hottest, has the lowest Eh and the lowest pH and evolves large quantities of H_2S. The relationships of pH and Eh to temperature may suggest that the primary waters are of sub-neutral pH. The elevated pH at lower temperature may be related to degassing of CO_2. The primary waters may also be reducing, although it is also conceivable that reducing, H_2S-rich conditions are imposed during the slow percolation of the water through biologically active sediments associated with the spring (unless the biota refreshes itself, however, this process is likely to be self-limiting).

Observation (2) suggests that the B, C and D springs represent re-emergences of the thermal waters after they have been subjected to a limited degree of dilution by surficial waters and/or shallow groundwaters and lost heat to the air and to the travertine mass.

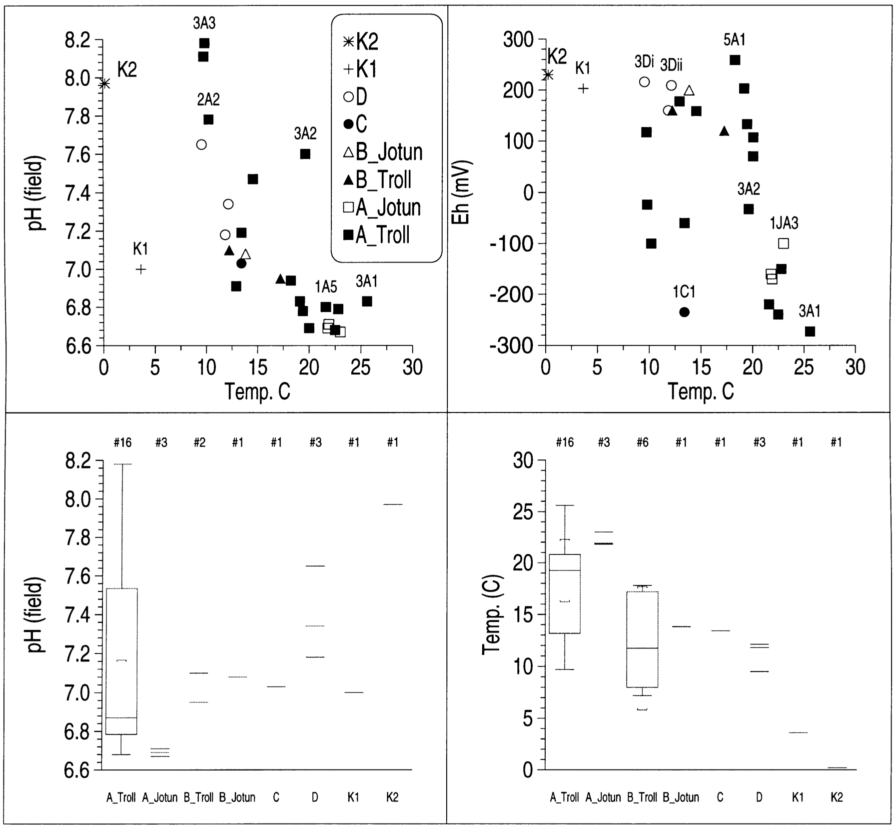

Fig. 5. Plots showing the relationship of temperature to Eh and pH, Bockfjord springs, Svalbard. In the box-plots of the lower two diagrams, the 'box' represents the interquartile range, with the median shown by a horizontal line. The whiskers represent the extraquartile data. Box-plots are not calculable for subsets of less than 5: in such cases the data points are shown as lines.

The Ca vs. Cl plot suggests that calcium is being attenuated by other processes than dilution, probably by calcite precipitation. The fact that neither Mg nor Sr exhibit a similar degree of attenuation is compatible with the lack of dolomite or strontianite in the XRD spectrum.

Observations (4), (10) and (11) suggest that the waters may be partially derived from a deep-seated saline thermal water whose composition in terms of Na, K, Si and SO_4 is determined by a water-rock equilibrium. Michard *et al.* (1996) suggest that sodium concentrations can be taken as a good indicator of the extent of water-rock interaction in thermal waters of the crystalline basement of Switzerland. The lesser degree of correlation of these parameters with Cl^- and the variability of the significant sodium–to–chloride excess (indicative of sodium derivation from silicate weathering — observation 5), suggest that chloride may not be wholly derived from water-rock interaction This hypothesis is supported by observation (7): Nordstrom *et al.* (1989), Michard *et al.* (1996) and Edmunds (1996) regard a Br/Cl ratio higher than seawater as being indicative of chloride-derivation from 'exotic' origins such as silicate water–rock interaction (fluid inclusions, radiogenesis), interaction with bromine-rich organic sediments or atmospheric pollution. The Br/Cl ratios

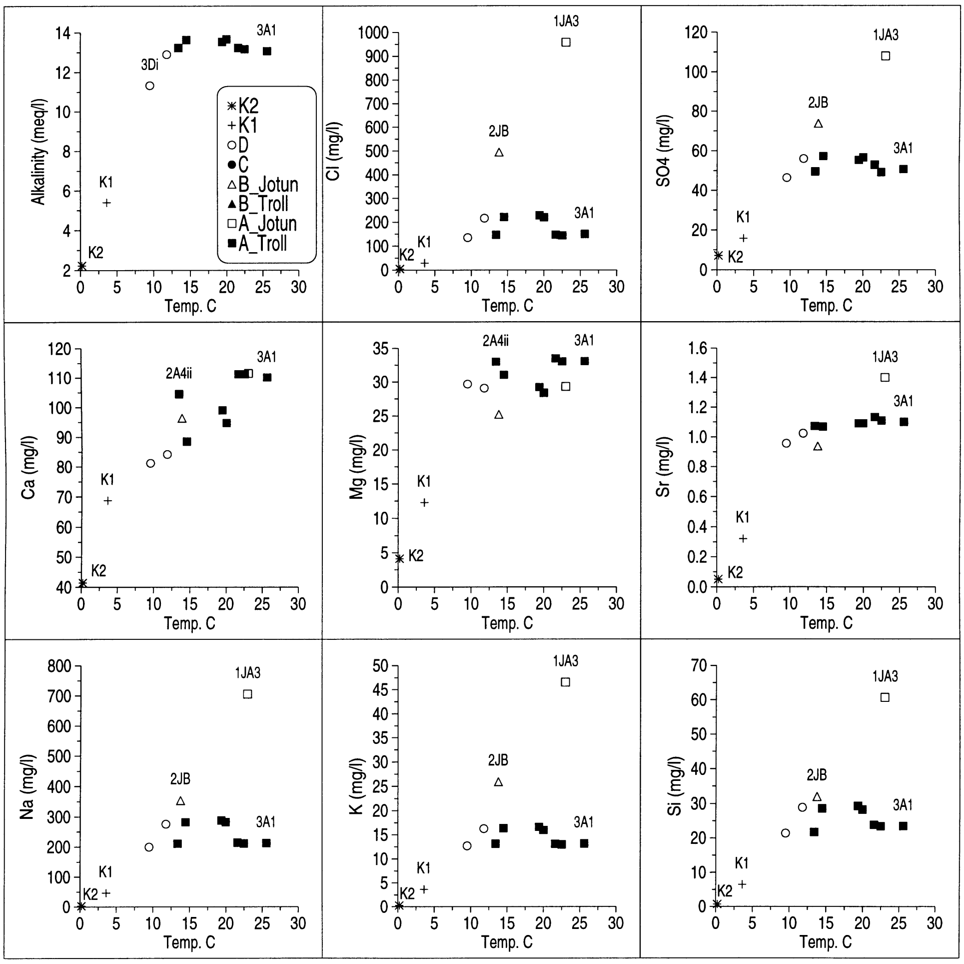

Fig. 6. Plots showing the relationship of selected parameters to temperature. In cases where the parameter is below the analytical detection limit, a value of half the detection limit is plotted.

found in the Svalbard springs indicate a slight bromide deficit relative to sea-water. Such a deficit may indicate at least partial derivation of chloride salinity from halite evaporites or conceivably preferential adsorption of bromide on organic matter (Edmunds, 1996). It is also conceivable that palaeo-seawater may have had a different Br/Cl ratio from that of today.

The lack of correlation of Ca, Mg, Sr and alkalinity with the well-correlated group Na, K and Si, suggests that concentrations of the former elements may have been modified either by dissolution from the higher level Hecla Hoek limestones exposed at the surface (rather than the rocks at depth, which are more likely to be siliceous) and/or by carbonate precipitation at high levels in the geothermal system.

Overall, the evidence suggests that the composition of the saline thermal waters may result from a (probably fossil) sea-water modified by water–rock interaction and dilution,

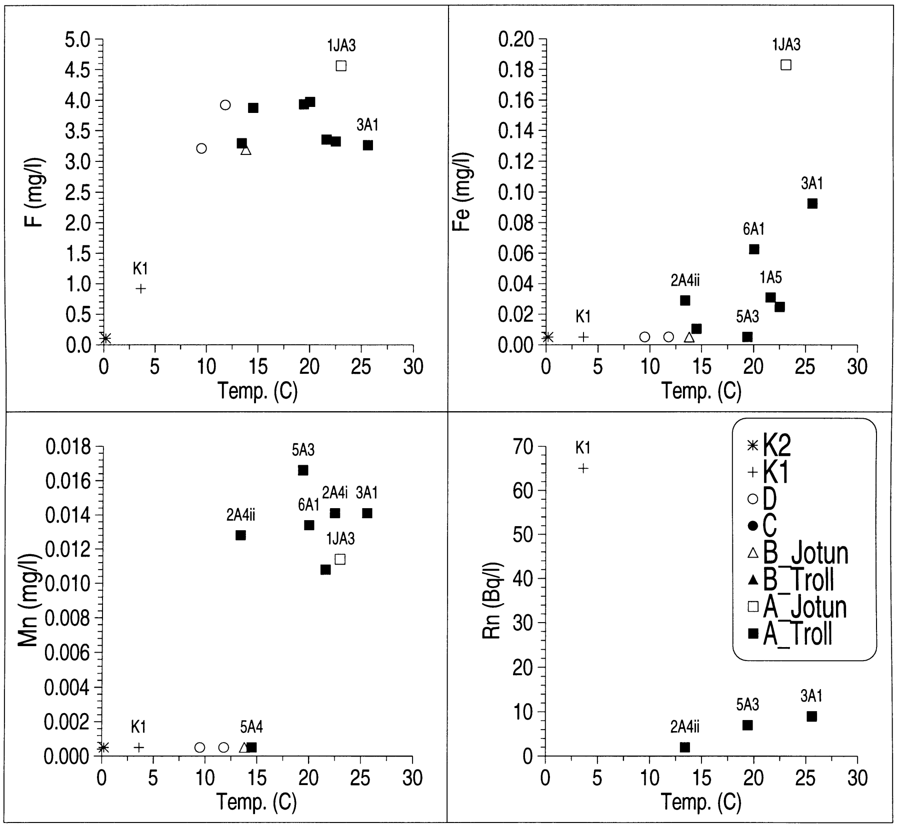

Fig. 7. Plots showing the relationship of selected parameters (F, Fe, Mn and Rn) to temperature. In cases where the parameter is below the analytical detection limit, a value of half the detection limit is plotted.

rather than purely from water–rock interaction. Another possibility is that the saline water may be derived from evaporite minerals. Evaporite deposits are not known on North Svalbard, but it cannot be excluded that they may exist at depth in the Devonian succession.

Geothermometry

At particular temperatures, common assemblages of minerals will tend towards equilibrium with a given water chemistry. Several researchers have noted that, for certain parameters or ratios of parameters, the relationship between temperature and composition will be stable and predictable. These parameters or ratios of parameters are known as geothermometers. In order for these to work, one has to assume that effects of dilution are insignificant and that thermodynamic equilibrium has been attained. In general, geothermometers based on ratios will be more resistant to dilution effects than those based on absolute concentrations. In addition, it should be realised that the temperature indicated by the geothermometer is not necessarily the maximum temperature of the water, but the

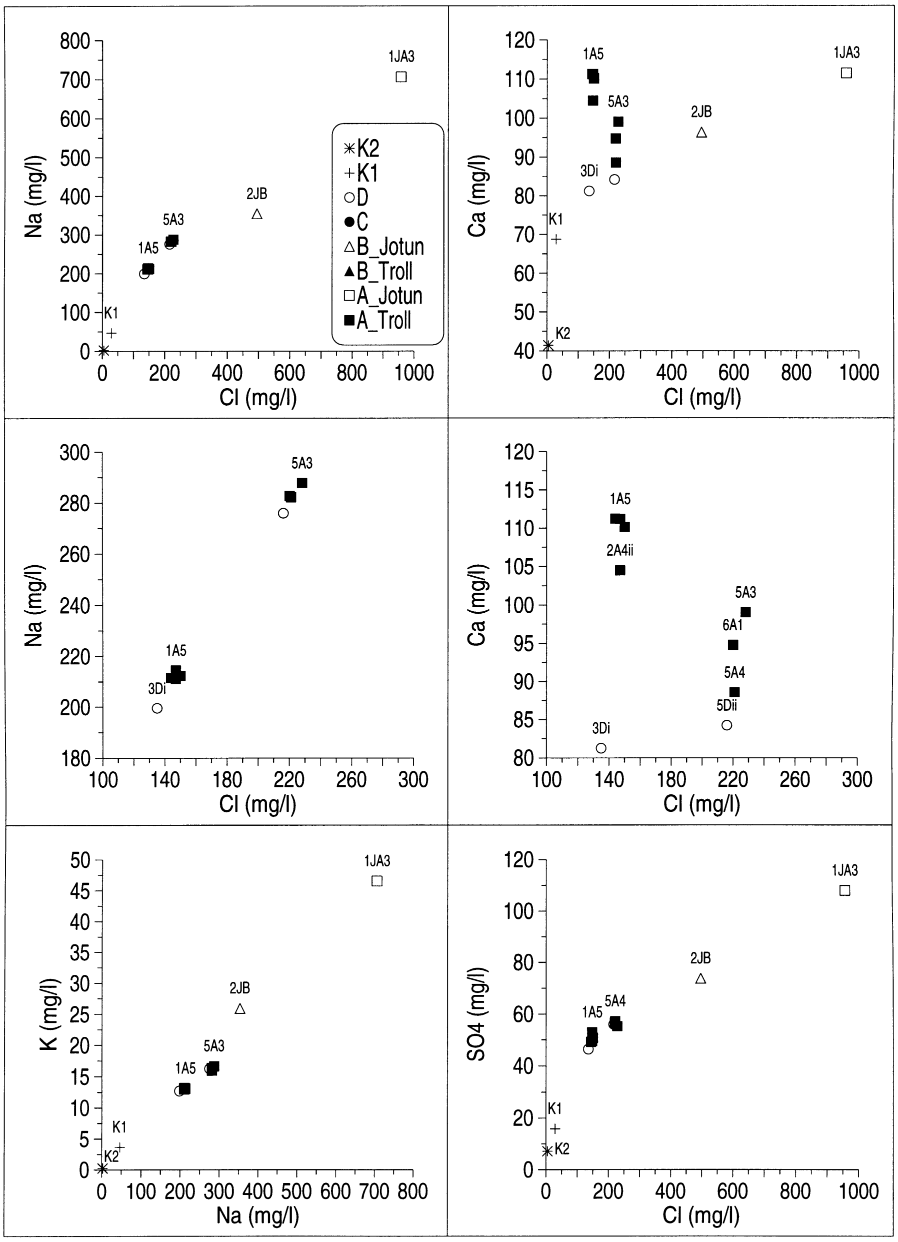

Fig. 8. Plots showing the relationship of selected major ions (Na, Ca and SO_4) to chloride, and of Na to K. In cases where the parameter is below the analytical detection limit, a value of half the detection limit is plotted.

temperature at which mineral and water phases were last in equilibrium with respect to the phases in question.

Several well-known geothermometers are summarised by Fournier (1981), who recom-

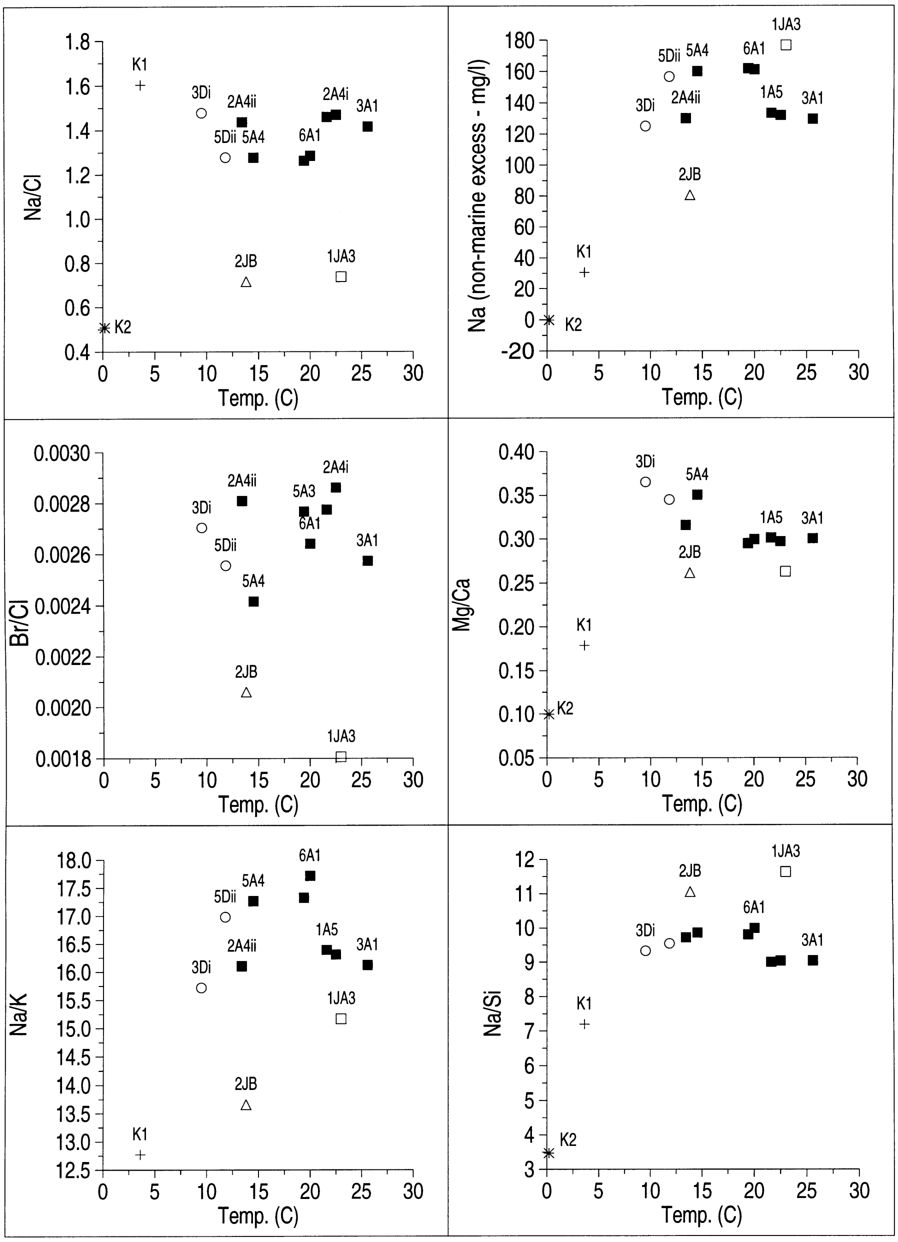

Fig. 9. Plots showing the relationship of selected mass ratios to temperature. In cases where one parameter of the ratio is below the analytical detection limit, no point is plotted. Symbols as in Fig. 8.

mends three as being particularly appropriate to most low-temperature thermal systems, namely the silica, the Na/K and the Na–Ca–K thermometers. Calculated results for these are shown in Table 3.

The quartz geothermometer can be corrected for dilution by the solution of simultaneous

Table 2. The chemical composition of the sampled springs in northern Svalbard

Spring	T (°C)	Alkalinity (meq/L)	Eh (mV)	pH	Rn (Bq/L) duplicates	F	Cl	Br	NO_3	SO_4	Si	Mg	Ca	Na	K	Fe	Mn	Ba	Sr	B	Li
1A5	21.6	13.2	−220	6.80		3.35	147	0.408	<0.05	52.9	23.8	33.5	111	214	13.1	0.031	0.011	0.112	1.1	0.226	0.350
2A4i	22.5	13.2	−240	6.68		3.32	144	0.412	<0.05	49.2	23.4	33.0	111	212	13.0	0.025	0.014	0.113	1.1	0.228	0.350
2A4ii	13.4	13.2	−60	7.19	<10 [2]	3.29	147	0.413	<0.05	49.5	21.7	33.0	104	211	13.1	0.029	0.013	0.107	1.1	0.218	0.346
3A1	25.6	13.1	−273	6.83	<10 [9, 8]	3.26	150	0.386	<0.05	50.7	23.5	33.1	110	212	13.2	0.093	0.014	0.112	1.1	0.212	0.348
3Di	9.5	11.3	216	7.65		3.21	135	0.365	0.18	46.4	21.4	29.7	81.3	200	12.7	<0.01	<0.001	0.097	0.96	0.210	0.324
5A3	19.4	13.5	133	6.78	<10 [7, 7]	3.93	228	0.631	0.21	55.3	29.3	29.2	99.0	288	16.6	<0.01	0.017	0.105	1.1	0.331	0.456
5A4	14.5	13.6	159	7.47		3.87	221	0.534	0.23	57.2	28.6	31.1	88.6	282	16.3	0.010	<0.001	0.096	1.1	0.325	0.454
5Dii	11.8	12.9	160	7.18		3.92	216	0.552	0.18	56.0	28.9	29.1	84.2	276	16.2	<0.01	<0.001	0.096	1.0	0.323	0.438
6A1	20.0	13.7	70	6.69		3.97	220	0.581	<0.05	56.6	28.3	28.4	94.8	283	16.0	0.063	0.013	0.110	1.1	0.311	0.443
1JA3	23.0	(10.4)	−100	6.67		4.56	958	1.73	<0.05	108	60.7	29.3	112	706	46.5	0.183	0.011	0.099	1.4	1.06	1.17
2JB	13.8	(7.3)	200	7.08		3.19	495	1.02	0.15	73.8	32.0	25.2	96.4	354	25.9	<0.01	<0.001	0.053	0.94	0.601	0.643
K1	3.6	5.4	203	7.00	65, 69	0.92	29.1	<0.1	0.23	15.8	6.5	12.3	68.8	46.7	3.7	<0.01	<0.001	0.037	0.32	0.045	0.071
K2	0.2	2.2	230	7.97		0.10	4.76	<0.1	<0.05	7.16	0.70	4.1	41.4	2.4	<0.5	<0.01	<0.001	0.008	0.051	<0.01	<0.005

All units are in mg/L unless otherwise stated. Values in rounded parentheses represent values calculated from the ionic balance. For radon determinations, a detection limit of 10 Bq/L is cited, although actual duplicate determinations (shown in square parentheses) indicate that this limit is probably too high.

Table 3. Calculated temperatures (°C) by the application of common geothermometers to sampled waters in northern Svalbard

Spring	T (°C)	Na/K Fournier (1981)	Na/K Truesdell (1976)	Quartz no steam loss	Chalcedony	Na–K–Ca ($\beta = 4.3$) Fournier and Truesdell (1973)	Na–K–Ca ($\beta = 1.3$) Fournier and Truesdell (1973)	T corr for Mg content Fournier and Potter (1979)	Na–K–Ca (corr.) Fournier and Potter (1979)
1A5	21.6	178	140	103	73	**78**	145	14	64
2A4i	22.5	178	140	102	72	**78**	145	13	65
2A4ii	13.4	179	141	98	68	**80**	146	18	62
3A1	25.6	179	141	102	72	**79**	146	14	64
3Di	9.5	181	143	98	67	**83**	149	29	55
5A3	19.4	174	135	113	84	**92**	148	31	61
5A4	14.5	174	135	111	82	**94**	149	41	53
5Dii	11.8	175	137	112	83	**95**	150	41	54
6A1	20.0	172	133	111	82	**92**	147	31	61
1JA3	23.0	184	147	152	127	142	**168**	104	64
2JB	13.8	192	156	117	88	112	**163**	103	60

The geothermometers used are those summarised by Fournier (1981). For the Na–K–Ca thermometer, the $\beta = 1/3$ value is used (bold type) if the $\beta = 4/3$ value is > 100°C. Temperatures are uncorrected for dilution.

equations for the effects of dilution on enthalpy and dissolved silica, using techniques described by Fournier and Truesdell (1974), or using the mixing diagram provided by Fournier (1981) as his Fig. 4.10. Such techniques applied to spring 3A1 yield temperatures of around 200°C for a deep, hot water comprising only 10–30% of the final spring water, following dilution by 70–90% by cold water of type K1 (Banks *et al.*, 1997a,b).

In summary, a combination of quartz (with dilution) and Na/K (not susceptible to dilution) geothermometers, suggests, at face value, that the Troll thermal springs are derived from a hot saline water of original temperature between 130 and 180°C, significantly diluted by cold groundwater during its passage to the surface (Banks *et al.*, 1997a,b). Given an average geothermal gradient of 0.079°C/m, the geothermometer temperatures correspond to a depth of some 1.6–2.3 km. Similar techniques used on the Jotun springs yield temperatures a few tens of degrees higher. The use of these geothermometers is, however, open to significant criticism on several counts, particularly in cool, aggressive, CO_2-rich waters such as these:

1. The Na–Ca–K thermometer (Fournier and Truesdell, 1973), and its magnesium correction (Fournier and Potter, 1979), is susceptible to disturbance by high-level dissolution of Mg and Ca from readily soluble carbonates of the Hecla Hoek marbles.
2. The Na–K thermometer may also be susceptible to interference from the same source (i.e. dissolution of Na and K from high-level marbles). In defence of the thermometer, the concentrations of Na and K in the marbles are very low (particularly in Sv5R, see Table 4), although the ratio Na/K is much lower in the marbles than the water. An Na/K fingerprint from the marbles on the waters would thus tend to artificially lower the aqueous Na/K ratio, resulting in misleadingly high calculated temperatures.
3. It may thus be suggested that the waters do not contain a particularly high-temperature component at all, but reflect waters circulating at shallow depths with little dilution. Nevertheless, dissolved silicon concentrations (using the chalcedony thermometer, which may be more appropriate for low T waters, Fournier, 1981) suggest minimum equilibration temperatures of at least 70°C for the Troll springs and 90–130°C for the Jotun springs, even without taking into account possible dilution. Even the chalcedony geothermometer is open to question, however, in cool, aggressive waters that are rich in CO_2. Such waters may attack silicate minerals other than quartz. Silicon concentrations may then accumulate in the water in concentrations greater than that reflecting quartz/chalcedony saturation (due to the slow kinetics of silica precipitation). Use of silica geothermometers in such situations will thus overestimate temperatures.

For the Bockfjord waters, geothermometers provide no unique interpretation. At face value, the most common thermometers suggest temperatures in excess of 130°C (with subsequent dilution by cold groundwaters), but it is likely that these overestimate real reservoir temperatures. The water chemistry may conceivably be compatible with a relatively shallowly circulating (a few hundred metres), cool geothermal system with relatively little dilution by non-geothermal groundwaters. This cool water may have acquired its aggressivity from volcanic CO_2 input and its salinity from a combination of water–rock interaction and admixture with a saline water/evaporite body.

Speciation and saturation modelling

The composition of the sampled spring waters was modelled using the code MINTEQA2. Iron and manganese redox couples were activated. Selected results of the modelling are

Table 4. X-Ray Fluorescence (XRF) analytical results for Mg, Ca, Na and Ca (as oxide %) for selected rock samples, and calculated molar and mass ratios

Sample no.	Rock type	MgO %	CaO %	Na_2O %	K_2O %	Mg/Ca molar	Na/K molar	Mg/Ca mass	Na/K mass
Sv1R	Fine-grained grey Hecla Hoek marble, Troll.	0.74	52.41	0.13	0.26	0.020	0.76	0.012	0.45
Sv5R	Fine-grained buff Hecla Hoek marble, Troll.	17.99	29.27	0.01	0.01	0.855	1.52	0.519	0.89
Sv17R	Coarser Hecla Hoek marble, Jotun.	0.75	52.62	0.29	0.07	0.020	6.29	0.012	3.70
Sv19R	Mica schist, Hecla Hoek, Jotun.	2.13	1.79	2.37	4.71	1.655	0.76	1.004	0.45
Sv28R	Devonian Old Red Sandstone, Troll.	0.87	2.05	0.34	1.51	0.590	0.34	0.358	0.20
Sv3R	Recent travertine—Troll area 5A4	0.84	50.91	0.11	0.03	0.023	5.57	0.014	3.28
Sv10R	Fossil travertine Troll area 1	1.13	51.77	0.13	0.1	0.030	1.98	0.018	1.16
Sv11Ra	Fossil travertine Troll area 3	0.67	54.23	0.09	0.01	0.017	13.67	0.010	8.04
Sv11Rb	Fossil travertine Troll area 3	1.01	53.79	0.1	<0.01	0.026	>15.2	0.016	>8.9
Sv14R	Fossil travertine—Troll area 7	0.77	53.43	0.05	0.05	0.020	1.52	0.012	0.89
Sv15R	Recent travertine—Troll area 3A2	0.55	52.58	0.2	0.02	0.015	15.19	0.009	8.94

Analyses performed by Ulrich Siewers at the Federal Institute for Geosciences and Natural Resources (BGR), Hannover, Germany.

indicated in Fig. 10a–c. In the following discussion, the term 'saturation' is used to apply to waters within ±0.3 of a saturation index (SI) of zero. The following features can be noted:

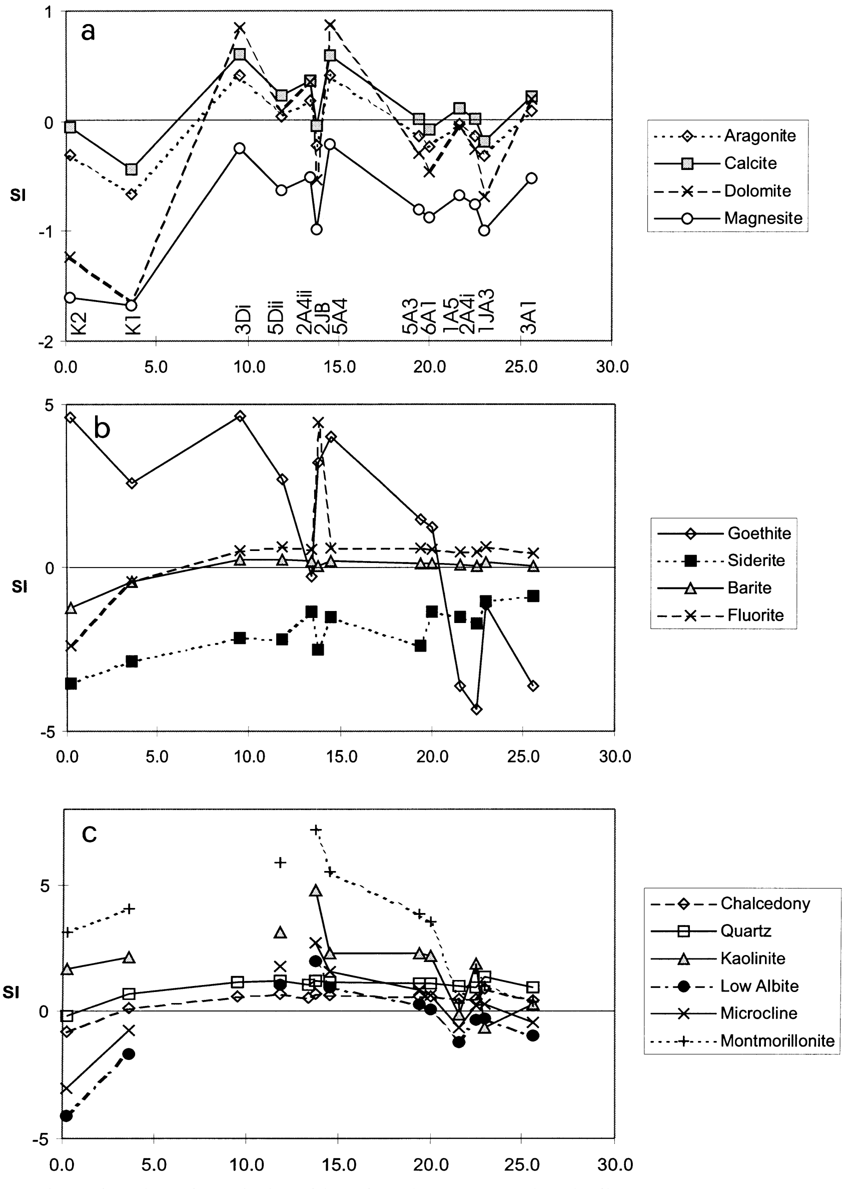

Fig. 10a–c. Plots showing the relationship of various saturation indices to temperature (°C; x-axis). In the few cases where a parameter is below the analytical detection limit, a value of half the detection limit has been used as input to MINTEQA2. In several samples where Al is below detection limit for ICP–AES, values derived from ICP–MS analyses carried out at BGR, Hannover, were used. The full ICP–MS data-set for a range of trace elements is reported by Banks *et al.* (1997b).

1. The thaw water K2 is saturated with respect to calcite and quartz, but significantly undersaturated with respect to dolomite, magnesite, strontianite, microcline, albite, anorthite, fluorite and barite. It is supersaturated with respect to goethite, kaolinite and montmorillonite. It is a typical shallow groundwater from a calcitic rock, where normal subaerial carbonate and silicate weathering processes are occurring.
2. The cold sub-permafrost groundwater K1 is saturated with respect to chalcedony, but supersaturated with respect to quartz, kaolinite, montmorillonite and goethite. The water is undersaturated with respect to calcite, dolomite, magnesite, strontianite, fluorite, barite, and the feldspar phases. The quartz oversaturation and calcite undersaturation are slightly unusual; the former may possibly be ascribed to mixing with a deeper, thermal water.
3. The hottest thermal water 3A1 is approximately saturated with respect to a number of mineral phases including kaolinite, microcline, aragonite, barite, calcite, dolomite. It is supersaturated with respect to fluorite, chalcedony and quartz and undersaturated with respect to the feldspar phases, magnesite and strontianite. These observations confirm that 3A1 is in approximate carbonate equilibrium with respect to dolomite and calcite (comprising the bulk of the surrounding dolomitic marble bedrock). The supersaturation with respect to the silica phases confirms the utility of these geothermometers, the precipitation of silica being kinetically slow relative to the implied rapid ascent of the thermal waters. The other hot ($>$ca 20°C) waters exhibit similar saturation features to 3A1.
4. The cooler thermal waters, which have presumably been subject to more dilution during their upward ascent or (in the case of the D springs) passage through the secondary travertine, tend towards a greater degree of supersaturation with respect to the carbonate and silicate minerals. The waters between 10 and 15°C tend to exhibit calcite, aragonite and dolomite supersaturation and in two cases magnesite saturation. These minerals are thus all candidates for possible deposition in travertine. XRD spectra indicate however that calcite is the unique detectable carbonate constituent in travertine samples. The cooler waters also tend to become supersaturated with respect to microcline and albite. The increasing saturation with respect to carbonate and silicate minerals can be ascribed to progressive degassing of carbon dioxide as water nears the surface environment, which leads to an increase in pH affecting the saturation of both silicate and carbonate phases. Phases such as quartz, chalcedony, fluorite and barite show little change in saturation status relative to the hot waters, the solubility of these minerals not being directly pH dependent.
5. The minerals gypsum, rhodochrosite, strontianite and siderite are undersaturated in all samples. The lack of strontianite saturation suggests that strontium is a mobile element and a useful indicator of water–rock interaction and dilution.

CONCLUSIONS

The Bockfjord thermal spring waters can be divided into three groups of similar ionic composition. Troll spring areas 1–3 yield waters of Na–(Ca)–HCO_3 composition, areas 5 and 6 waters of Na–HCO_3 composition, and the Jotun springs waters of Na–Cl composition. There is a negative correlation between temperature and Eh, and temperature and pH. The warmest water, at 25.6°C, has an Eh of -270 mV, a pH of 6.83 and contains hydrogen sulphide. It is thus suggested that the 'pristine' thermal water source has a sub-neutral pH and may be reducing (although the low Eh may alternatively result from biological activity in near-surface sediments). The thermal waters are also likely to be CO_2-bearing; although no gas samples were taken, the negative relationship of pH and temperature is indicative of degassing of CO_2.

Common geothermometers yield widely varying temperatures for the thermal water source. The most likely solutions, taken at face value, suggest derivation from hot, saline water bodies at depth with temperatures of 130–180°C for the Troll springs, with 10–30% thermal, saline water diluted by 70–90% cold water. This corresponds to a depth of 1.6–2.3 km. The Jotun springs appear to be derived from a thermal water source some few tens of °C hotter. The geothermometers are fraught with difficulties, however, and a shallow (several hundred metres depth), relatively cool geothermal system (possibly charged with volcanic CO_2 and admixing with a saline source) may not be incompatible with the hydrogeochemistry.

Br/Cl ratios suggest that the chloride salinity of the water is not wholly derived from water–rock interaction but rather from fossil sea-water or, conceivably, evaporitic deposits in the Devonian sandstones. The sodium, potassium, sulphate and silicon concentrations appear to be controlled by near-equilibrium water–rock interactions within the geothermal aquifer.

Acknowledgements—Field work at Bockfjord was funded by a grant from the Research Council of Norway to the Agricultural University of Norway. The Norwegian Polar Institute was responsible for the logistics of the expedition to Bockfjord. ICP–MS analyses of Al (see Fig. 10) and XRF analyses of marbles were provided by Dr. Ulrich Siewers of the Federal Institute for Geosciences and Natural Resources (BGR), Hannover, Germany. Radon analyses were kindly carried out by Prof. Terje Strand and colleagues at the Norwegian Radiation Protection Authority. We would like to thank the Governor of Svalbard for granting permission for our work in the National Park of Northern Spitsbergen.

REFERENCES

Amundsen, H. E. F., Griffin, W. L. and O'Reilly, S. Y. (1988) The nature of the lithosphere beneath northwestern Spitsbergen: xenolith evidence. In *Progress in Studies of the Lithosphere in Norway*, ed. Y. Kristoffersen, Norges Geologiske Undersøkelse Special Publication, **No. 3**, pp. 58-65.

Banks, D., Siewers, U., Sletten, R.S., Haldorsen, S., Dale, B., Heim, M., Swensen, B. and Siewers, U. (1997a) The world's northernmost thermal springs? Trollkildene and Jotunkildene, Bockfjord, Svalbard [extended abstract]. *Norges Geologiske Undersøkelse Bulletin*, **433**, 60–61.

Banks, D., Siewers, U., Sletten, R.S., Haldorsen, S., Dale, B., Heim, M. and Swensen, B. (1997b) The Bockfjord thermal springs of Svalbard: data report. *Norges Geologiske Undersøkelse Rapport*, **97**.183, 112 pp.

Edmunds, W. M. (1996) Bromine geochemistry of British groundwaters. *Mineralogical Magazine* **60**, 275–284.

Fournier, R. O. (1981) Application of water geochemistry to geothermal exploration and reservoir engineering. In *Geothermal Systems: Principles and Case Histories*, ed. L. Rybach and L. J. P. Muffler, pp. 109–143. John Wiley and Sons.

Fournier, R. O. and Truesdell, A. H. (1973) An empirical Na-K-Ca geothermometer for natural waters. *Geochimica et Cosmochimica Acta* **37**, 1255–1275.

Fournier, R. O. and Truesdell, A. H. (1974) Geochemical indicators of subsurface temperature - part 2, estimation of temperature and fraction of hot water mixed with cold water. *Journal of Research of the United States Geological Survey* **2**, 263–270.

Fournier, R. O. and Potter, R. W. (1979) Magnesium correction to the Na-K-Ca geothermometer. *Geochimica et Cosmochimica Acta* **43**, 1543–1550.

Gee, D.G. and Moody-Stuart, M. (1966) The base of the Old Red Sandstone in central north Haakon VII Land, Vestspitsbergen. *Norsk Polarinstitutt, Årbok* **1964**, 57–68.

Gjelsvik, T. (1979) The Hecla Hoek ridge of the Devonian graben between Liefdefjorden and Holtedahlfonna, Spitsbergen. *Norsk Polarinstitutt Skrifter* **167**, 63–71.

Haldorsen, S. and Lauritzen, S. E. (1993) Subpermafrost groundwater in Svalbard. In *Hydrogeology of Hard Rocks*, ed. S.B. Banks and D. Banks, pp. 940-949. Memoirs of the XXIVth Congress of the International Association of Hydrogeologists, NGU, Trondheim, Norway, pp. 940–949.

Hjelle, A. (1993) *Geology of Svalbard.* Polarhåndbok No. 7, Norsk Polarinstitutt, Oslo, 163 pp.

Hoel, A. (1914) Nouvelles observations sur la district volcanique du Spitsberg du nord. *Videnskapsselskapets skrifter* (*Christiania*), *Matematikk*, *Naturvernklasse*, **No. 9**, (Oslo).

Hoel, A. and Holtedahl, O. (1911) Les nappes de lave, les volcans et les sources thermales dans les environs de la baie Wood au Spitsberg. *Videnskapsselskapets skrifter* (*Christiania*), *I. Matematikk*, *Naturvernklasse*, **No. 8**, 37 pp. (Oslo).

Hoel, A. and Holtedahl, O. (1913) Lavadækkerne, vulkanerne og de varme kilder ved Wood Bay paa Spitsbergen. *Naturen* **37**, 3–19, (Oslo).

Horne, R. A. (1969) *Marine Chemistry*. Wiley Interscience.

Langangen, A. (1979) *Chara canascens* reported from Spitsbergen. *Phycologia* **18**, 436–437.

Lauritzen, S. E. (1991) Groundwater in cold climates: interaction between glacier and karst aquifers. In *Arctic Hydrology. Present and Future Tasks*, ed. Y. Gjessing, J.O. Hagen, K.A. Hassel, K. Sand and B. Wold, Norwegian National Committee for Hydrology, Report No. 23, pp. 139-146. Oslo.

Lauritzen, S. E. and Bottrell, S. (1994) Microbiological activity in thermoglacial karst springs, South Spitsbergen. *Geomicrobiology Journal* **12**, 161–173.

Liestøl, O. (1976) Pingoes, springs and permafrost in Spitsbergen. *Norsk Polarinstitutts Årbok* **1975**, 7–29.

Michard, G., Pearson, F. J. and Gautschi, A. (1996) Chemical evolution of waters during long-term interaction with granitic rocks in northern Switzerland. *Applied Geochemistry* **11**, 757–774.

Nordstrom, D. K., Ball, J. W., Donahoe, R. J. and Whittemore, D. (1989) Groundwater chemistry and water-rock interactions at Stripa. *Geochimica et Cosmochimica Acta* **53**, 1727–1740.

Orvin, A. K. (1944) Litt om kilder på Svalbard. *Norsk Geografisk Tidsskrift* **10**, 16–37.

Reimann, C., Hall, G. E. M., Siewers, U., Bjorvatn, K., Morland, G., Skarphagen, H. and Strand, T. (1996) Radon, fluoride and 62 elements as determined by ICP-MS in 145 Norwegian hard rock groundwater samples. *The Science of the Total Environment* **192**, 1–19.

Skjelkvåle, B. L., Amundsen, H. E. F., O'Reilly, S. Y., Griffin, W. L. and Gjelsvik, T. (1989) A primitive alkali basaltic stratovolcano and associated eruptive centres, Northwestern Spitsbergen: volcanology and tectonic significance. *Journal of Volcanology and Geothermal Research* **37**, 1–19.

Truesdell, A. H. (1976) Summary of Section III - Geochemical techniques in exploration. *Proc.* 2^{nd} *United Nations Symposium on the Development and Use of Geothermal Resources, San Francisco, USA*, May 1975, **1**, pp. liii–lxiii.

Vågnes, E. and Amundsen, H. E. F. (1993) Late Cenozoic uplift and volcanism on Spitsbergen; caused by mantle convection? *Geology* **21**, 251–254.

Ødegård, M. and Andreassen, B. T. (1987) Methods for water analysis at the Geological Survey of Norway. In *Geomedical Consequences of the Chemical Composition of Freshwater*, pp. 133-150. Norwegian Academy of Science and Letters.